Polar head group interactions in mixed Langmuir monolayers

P. Viswanath and K. A. Suresh*
Raman Research Institute, Sadashivanagar, Bangalore, 560 080, India
(Received 10 December 2002; revised manuscript received 12 March 2003; published 25 June 2003)

We have investigated the miscibility in the mixed monolayers of cholesterol (Ch)-octyl cyano biphenyl (8CB) and cholesteryl acetate (ChA)-8CB using surface manometry and epifluorescence microscopic techniques. The main skeleton is the same both in Ch and ChA, whereas the polar head group is alcohol in Ch and ester in ChA. The 8CB molecule has a polar cyano as a terminal group and we probe its interaction with the polar group of Ch or ChA molecules in the mixed monolayers. Both Ch-8CB and ChA-8CB mixed monolayers exhibit two collapse pressures. In the case of the Ch-8CB mixed monolayer, the lower collapse pressure varies after 0.6 mole fraction (MF) of Ch in 8CB and the higher collapse pressure is nearly independent of composition. In ChA-8CB mixed monolayer, the lower collapse pressure varies continuously with the composition of ChA while the higher collapse pressure is nearly independent of the composition of ChA. In both these mixed monolayers, above the lower collapse pressure, 8CB gets squeezed out of the monolayer and forms multilayers. We find that in the case of Ch-8CB there is a phase separation in the monolayer occurring in the range of 0.15–0.9 MF of Ch. However, in ChA-8CB, the monolayer phase is miscible in all the proportions (except at very high concentration of ChA) below the lower collapse pressure. We attribute this better miscibility in the ChA-8CB compared to the Ch-8CB to the role played by the ester and cyano polar head group interactions.

DOI: 10.1103/PhysRevE.67.061604 PACS number(s): 68.37.−d, 64.75.+g, 68.18.−g

I. INTRODUCTION

Mixed Langmuir monolayers are of considerable interest as model systems to mimic biological membranes [1]. Studies on mixed monolayers will provide information about the interactions involved, miscibility, and stability of the monolayer [2]. It is known that cholesterol (Ch) is found in bilayer plasma membranes and lipoproteins. It regulates the transport and barrier properties of the membrane [3]. There have been extensive studies on the mixed monolayers of cholesterol and lipids. The mixed monolayers of Ch and oleic acid show good miscibility. This is attributed to the Ch molecules filling the voids in the monolayer of oleic acid, which are bent molecules [4]. With stearyl alcohol, which is linear, Ch is not miscible and gives rise to inhomogeneous monolayer [5]. The miscibility of Ch is not good in the case of stearic acid which is also linear [6]. These studies indicate that the miscibility in a mixed monolayer depends mainly on the shape of the constituent molecules. Studies on the Ch and phospholipid mixed monolayers indicate a good miscibility [7–9]. These studies consider the interaction of the acyl chain with Ch rigid skeleton. It is found that the rigid hydrophobic skeleton of cholesterol stiffens the acyl chains of lipid [10] affecting the barrier properties of the membrane. The role played by the carbonyl oxygens of phospholipid with Ch has also been addressed considering the possibilities of the hydrogen bond formation between them [11].

In this paper, we report our studies on the miscibility in mixed monolayers of Ch-octyl cyanobiphenyl (8CB) and cholesteryl acetate (ChA)-8CB. We have probed the interaction of the polar group of Ch with the polar group of a linear molecule such as 8CB. For comparison, we have also probed the interaction of a weakly polar group of ChA molecule with 8CB. Here the interaction between the rigid skeleton of Ch and biphenyl core of 8CB is minimum and this allows us to investigate the polar (head group-head group) interactions. This is also valid in the case of ChA. The CN group of 8CB has a dipole moment of around 4 Db [12] leading to a strong dipole-dipole repulsion between the molecules in the 8CB monolayer. This repulsion results in the tilting of the biphenyl core of the 8CB molecules by 60° to the normal at the air-water (A-W) interface giving rise to a limiting area per molecule (A/M) of 48 $Å^2$. This is almost twice the A/M of single benzene ring oriented perpendicular to the A-W interface [13]. We have employed the surface manometry and epifluorescence microscope techniques to study the interactions of OH polar group of Ch or OCO polar group of ChA with the CN polar group of 8CB molecules. Our results showed that in the Ch-8CB mixed monolayer Ch is immiscible with 8CB except at very low and very high mole fractions (MF) of Ch. The polar group interactions of Ch and 8CB lead to a phase separation. Our studies indicated that the separated phases were 8CB rich phase and Ch rich phase. We infer that the former is in the L_1 phase. In the literature, L_1 is also referred as liquid expanded or low density liquid where a fluorescent dye partitions easily, thereby the phase appears bright under the epifluorescence microscope [14,15] and the latter is in the L_2 phase, i.e., condensed monolayer phase. (The condensed phase is a high density phase. In the literature [16], many variants of the condensed phase have been reported. Here, the dye separates out and the phase appears dark under the epifluorescence microscope.) Interestingly, in the case of ChA-8CB, the interactions between the less polar OCO group of ChA and CN groups of 8CB lead to a miscible mixed monolayer for almost all proportions.

II. EXPERIMENT

Cholesterol and cholesteryl acetate were obtained from Aldrich and recrystallized using ethanol and butanone sol-

*Electronic address: suresh@rri.res.in

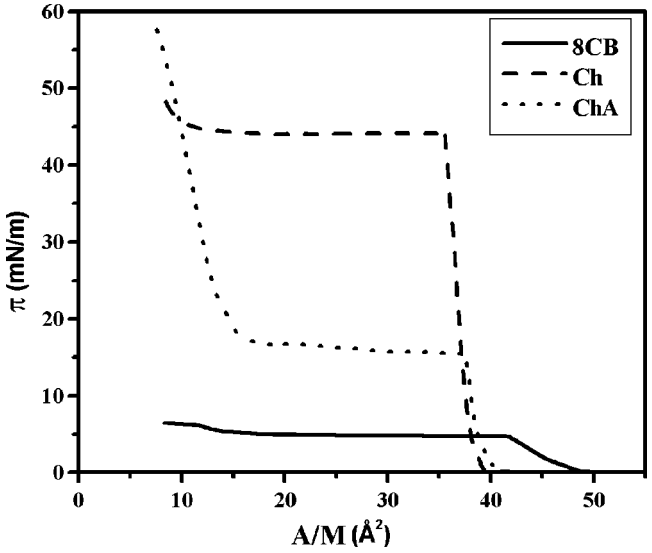

FIG. 1. Surface pressure π-area per molecule (A/M) isotherms of 8CB, Ch, and ChA monolayers at temperature $t=22$ °C. The compression rate was 0.02 (Å^2/molecule)/s.

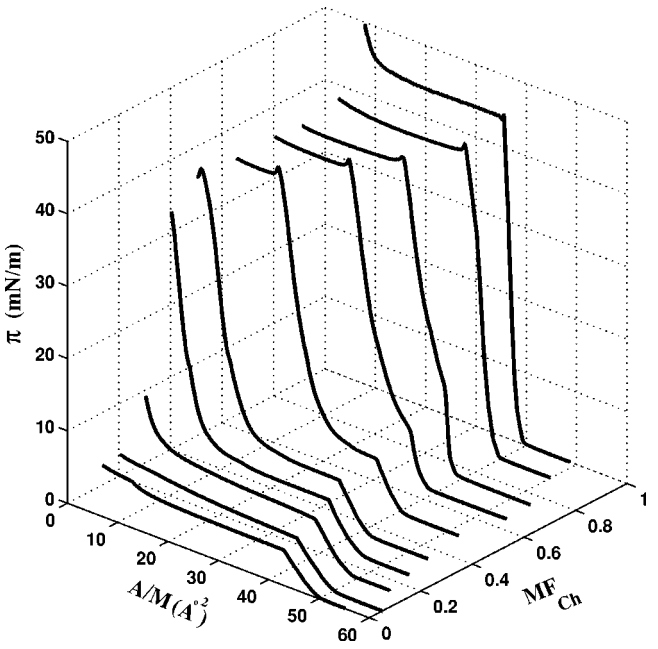

FIG. 2. Surface pressure π-area per molecule (A/M) isotherms for mixed monolayers at different mole fractions (MF) of Ch in 8CB at $t=22$ °C.

vents, respectively. Octyl cyano biphenyl (Aldrich) was used as procured. The surface manometry experiments were carried out using NIMA 611M trough. The subphase used was Millipore water (resistivity >18.2 MΩ cm) whose temperature t was maintained around 22 ± 0.5°C unless otherwise specified. The relative humidity was about $(85\pm5\%)$. Stock solution of concentration 1.5 mM was prepared and used for making mixtures of required composition. The monolayer was spread using a microsyringe (Hamilton) and was equilibrated for 10 min to allow the solvent to evaporate. The monolayer was compressed at the rate of 0.02 (Å^2/molecule)/s. Epifluorescence microscopy was used to characterize the various phases indicated by the surface pressure area-per molecule isotherms. For these studies, a fluorescent dye 4-(hexadecylamino)-7-nitrobenz-2 oxa-1,3 diazole (Molecular Probes) of about 0.5% molar concentration was added to the mixture. The monolayer doped with this dye was directly observed under a Leitz Metallux 3 microscope. The images were obtained using a photon intensified charge coupled device camera (Model P 46036A/V22, EEV) and was captured using a NI (PCI-1411) frame grabber for analyzing.

III. RESULTS

The surface pressure, π-area per molecule (A/M) isotherms of the individual Ch, ChA, and 8CB are shown in Fig. 1. Cholesterol monolayer exhibits the following phase sequence. Above an A/M of 40 Å^2, the surface pressure is almost zero, indicating gas (G) + condensed phase coexistence. On compressing the monolayer there was a steep increase in the surface pressure at 40 Å^2 indicating the onset of a condensed phase. On further compression, the monolayer, collapsed at a surface pressure of 44.6 mN/m. The isotherm yields the limiting value of A/M to be 38.3 Å^2. After the collapse, the isotherm has a plateau region, which extends up to 17 Å^2. Thereafter the surface pressure again increased gradually. The ChA has a similar isotherm although the collapse pressure of ChA is 15.4 mN/m. The limiting value of A/M is 39.2 Å^2. We denote the condensed phase of Ch and ChA as L_2 phase based on our epifluorescence studies and other reports in the literature [17]. The isotherm of 8CB exhibits the sequence of a coexisting $G+L_1$ phase, L_1 phase, coexisting L_1 + three layer (D_1) phase and a coexisting L_1+D_1 + multilayer (D_2) phase. These isotherms were in good agreement with the earlier reports on Ch [17], ChA [18], and 8CB [19,20].

The π-(A/M) isotherms for the mixed monolayer of Ch-8CB are shown in Fig. 2. The isotherms for the mixed monolayer exhibit two collapse pressures. The lower collapse pressure is characteristic of 8CB and is denoted by $\pi_{c(8CB)}$. The higher collapse pressure characteristic of Ch is denoted by $\pi_{c(Ch)}$.

The π-(A/M) isotherms of ChA-8CB mixtures are shown in Fig. 3. Here also the presence of two collapse pressures is seen. The lower collapse pressure is denoted by $\pi_{c(8CB)}$ and the higher collapse pressure is denoted by $\pi_{c(ChA)}$.

The epifluorescence studies of pure Ch [21] and pure 8CB [14] have already been reported and our results are in agreement with them.

However, we are not aware of any epifluorescence microscopic studies on the monolayer of ChA. Our epifluorescence studies on ChA showed some interesting features in the $G+L_2$ region of the isotherm Fig. 4. At very large A/M of 134.5 Å^2, we could observe the usual circular ''gas'' domains, which appeared black. They were coexisting with the L_2 phase. The L_2 phase appeared as a bright and black mesh texture within a big domain as shown in Fig. 4(a). These L_2 domains possessed irregular boundaries. On compression,

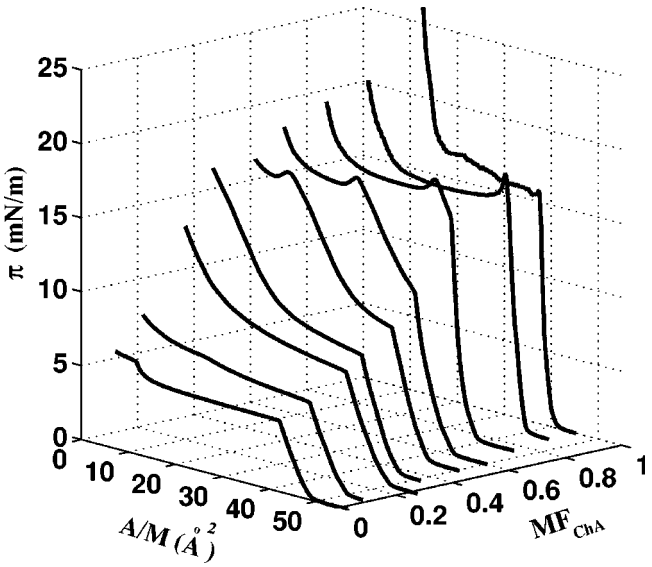

FIG. 3. Surface pressure π-area per molecule (A/M) isotherms for mixed monolayers at different MF of ChA in 8CB at $t = 22$ °C.

the gas domains disappeared and gave rise to only L_2 phase Fig. 4(b). Above $\pi_{c(\mathrm{ChA})}$, the crystallites of ChA were seen to coexist with L_2 phase.

For the Ch-8CB mixtures, we have carried out epifluorescence studies at various mole fractions of Ch. The epifluorescence images obtained for 0.5 MF of Ch in Ch-8CB mixtures are shown in Fig. 5. The mixed monolayer exhibited clearly the $G+L_1+L_2$ coexisting phase [Figs. 5(a) and 5(b)], which was followed by L_1+L_2 phase. The L_1 and L_2 were well separated phases. The L_1 domains were brighter compared to the L_2 domains. At higher pressures, the L_1 phase covered a larger region [Fig. 5(c)]. Above $\pi_{c(8\mathrm{CB})}$, the L_1 phase transformed into a three layer (D_1) phase and coexisted with the L_2 phase [Fig. 5(d)]. At still higher pressures, in the steep region of the isotherm, most of the D_1 domains transformed into multilayer (D_2) domains and coexisted with L_2 phase [Fig. 5(e)]. Above $\pi_{c(\mathrm{Ch})}$, the L_2 phase transformed to crystallites of Ch which coexisted with D_2 domains [Fig. 5(f)].

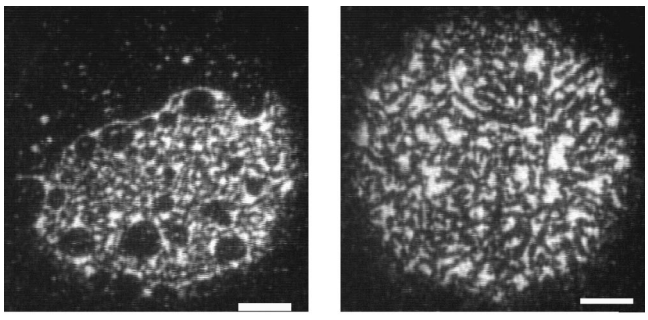

FIG. 4. Epifluorescence images of cholesteryl acetate at the A-W interface. Figure (a) shows the coexistence of circular gas domains (black) with L_2 phase which appeared as a bright and black mesh texture within a big domain. Figure (b) shows the absence of gas phase and the presence of only L_2 phase (bright and black mesh texture) at lower A/M. Scale bar represents 50 μm.

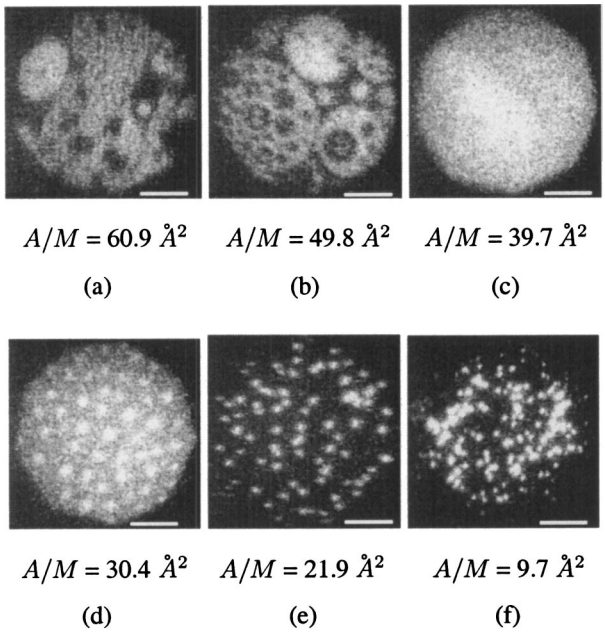

FIG. 5. Epifluorescence images at 0.5 mole fraction of Ch in the Ch-8CB mixed monolayer at the A-W interface. In figures (a) and (b), $G+L_1+L_2$ coexistence phases are clearly seen. Here the brighter domains [top left corner in (a) and top region in (b)] represent 8CB rich L_1 phase. The other less bright domains represent Ch rich L_2 phase. The dark region represents the gas phase. Figure (c) shows the predominant L_1 phase coexisting with L_2 phase. Figure (d) shows the bright D_1 domains embedded in the L_2 phase background. Figure (e) shows the coexistence of L_2+D_2 phase. Here the D_2 domains are much brighter and in contrast the L_2 phase in the background appeared dark. Figure (f) shows the collapsed state of Ch crystallites (dark background) coexisting with D_2 phase. Scale bar represents 50 μm.

The epifluorescence images of 0.75 MF of Ch in the Ch-8CB mixed monolayer are shown in Fig. 6. At this composition the mixed monolayer exhibits the $G+L_1+L_2$ coexistence phase [Fig. 6(a)], which on compression yields the L_1+L_2 coexistence phase [Figs. 6(b) and 6(c)]. Above $\pi_{c(8\mathrm{CB})}$, the D_2 domains were seen to nucleate from the L_1 phase [Fig. 6(d)], which indicated that the L_1 phase was 8CB rich. The onset of the D_2 phase from the L_1 phase corresponded to the kink in the isotherm at 0.75 MF. Unlike in the case of 0.5 MF of Ch, here, the L_1 domains straightaway transformed into D_2 domains. At the collapse pressure $\pi_{c(\mathrm{Ch})}$, the L_2 phase transformed into Ch crystallites, which indicated that the L_2 phase was Ch rich. The Ch crystallites coexisted with the multilayer D_2 phase as shown in Figs. 6(e) and 6(f). Based on the detailed epifluorescence and surface manometry studies, a phase diagram was constructed for the Ch-8CB mixed monolayer. This is shown in Fig. 7.

The epifluorescence studies for the ChA-8CB mixed monolayer were also carried out at various proportions of ChA. Figure 8 shows the images obtained for 0.5 MF of ChA in the ChA-8CB mixed monolayer. Here we observed the $G+L_1$ coexistence phase followed by the L_1 phase. The L_1

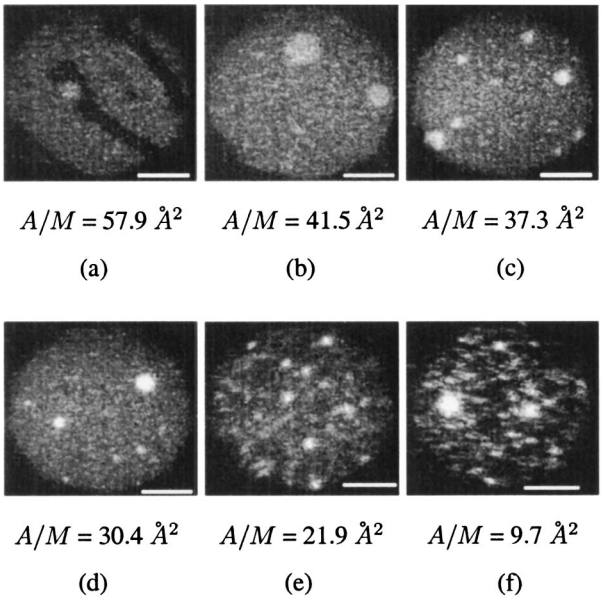

FIG. 6. Epifluorescence images at 0.75 mole fraction of Ch in the Ch-8CB mixed monolayer at the A-W interface. Figure (a) shows the $G+L_1+L_2$ coexistence phase. Here the black stripe represents the gas phase, the single brighter domain is the L_1 phase, and the background is the L_2 phase. Figures (b) and (c) show the bright L_1 domains and the background L_2 in coexistence. Figure (d) represents the coexistence of L_2 (background) and D_2 domains (very bright). Figures (e) and (f) shows the D_2 domains (very bright) coexisting with crystallites of Ch (dark background) in the collapsed state. Scale bar represents 50 μm.

phase was uniformly bright and did not indicate any phase separation. On further compression, the L_1 phase collapsed at $\pi_{c(8CB)}$. Above this surface pressure, the L_1 phase coexisted with the D_2 multilayer phase [Figs. 8(a) and 8(b)]. At $\pi_{c(ChA)}$, the L_1 phase transformed into ChA crystallites. Here the D_2 phase coexisted with the ChA crystallites [Fig. 8(c)]. This trend was observed up to 0.95 MF of ChA. A phase diagram of the ChA-8CB mixed monolayer obtained from our studies is shown in Fig. 9. The variation of collapse pressure with increasing MF of Ch in 8CB is shown in Fig. 10. There were two collapse pressures in the isotherm for the mixed monolayer. The lower collapse pressure $\pi_{c(8CB)}$ which was invariant up to 0.6 MF of Ch, steeply rose for higher MF of Ch. The higher collapse pressure $\pi_{c(Ch)}$ did not vary with the composition of Ch.

The collapse pressure as a function of the MF of ChA in 8CB is shown in Fig. 11. Here again there were two collapse pressures in the isotherm. Interestingly, in this mixture, the lower collapse pressure $\pi_{c(8CB)}$ continuously increased with the concentration of ChA. The higher collapse pressure $\pi_{c(ChA)}$ was independent ot the composition of ChA.

To analyze the degree of miscibility in the ChA-8CB

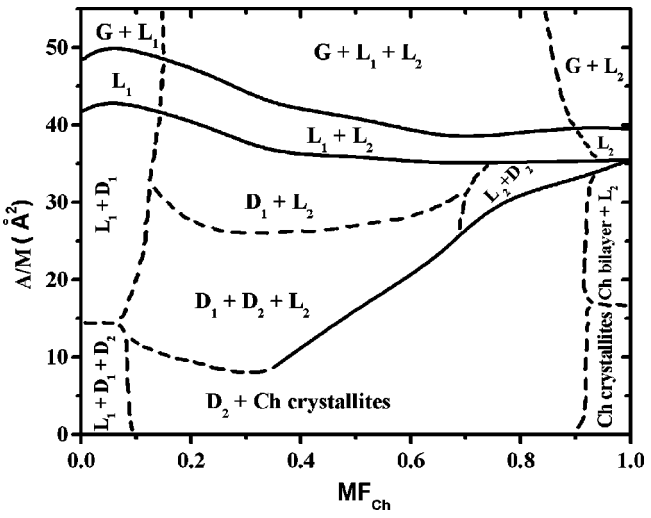

FIG. 7. Phase diagram of Ch-8CB mixed monolayers at $t=22$ °C. Here, the continuous lines indicate the actual phase boundaries and the dashed lines indicate the approximate phase boundaries.

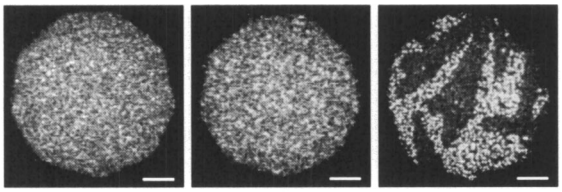

FIG. 8. Epifluorescence images at 0.5 mole fraction of ChA in ChA-8CB mixed films at the A-W interface. Figures (a) and (b) represent the L_1+D_2 phase coexistence. Here the small but brighter D_2 domains are coexisting with the background L_1 phase. As one goes from (a) to (b), the D_2 domains became bigger. Figure (c) shows the collapsed state of the L_1 phase as ChA crystallites coexisting with D_2 domains. The ChA crystallites appeared dark in contrast with the much brighter D_2 domains. Scale bar represents 50 μm.

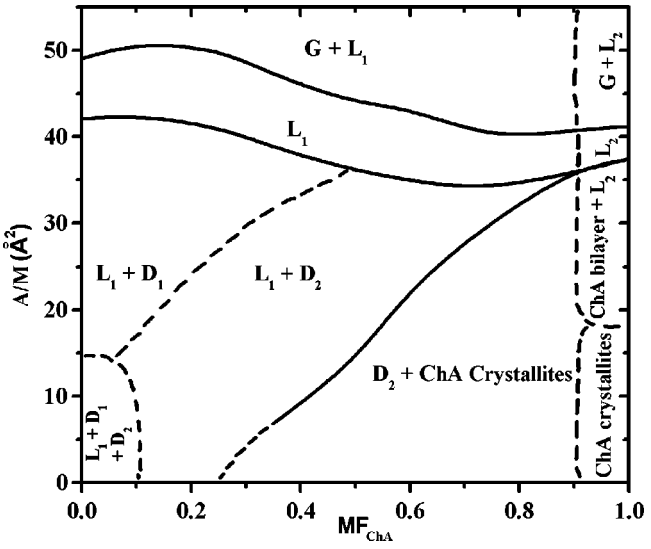

FIG. 9. Phase diagram of ChA-8CB mixed monolayers at $t=22$ °C. Here, the continuous lines indicate the actual phase boundaries and the dashed lines indicate the approximate phase boundaries.

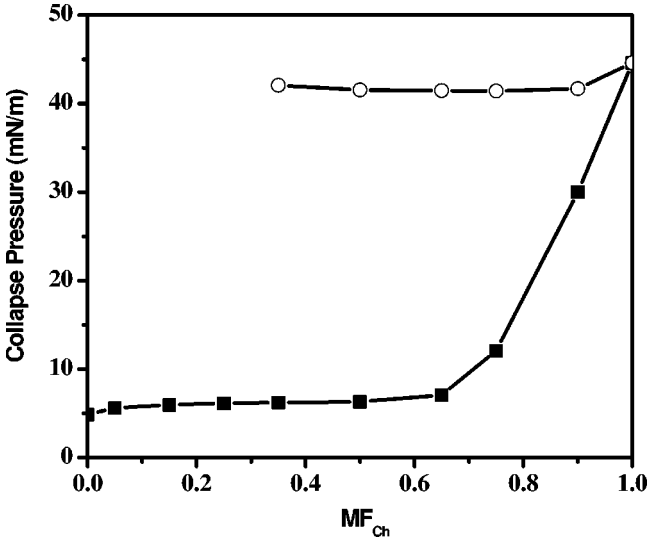

FIG. 10. Variation of collapse pressure as a function of the mole fraction of Ch in Ch-8CB mixed monolayers. The open circles represent the higher collapse pressure $\pi_{c(\mathrm{Ch})}$. The filled squares represent the lower collapse pressure $\pi_{c(8\mathrm{CB})}$.

mixed monolayer, we have calculated the excess area and Gibbs free energy. For the ideal case of either complete miscibility or complete immiscibility, the law of additivity of areas is given by [2,22],

$$A_{id}=A_1X_1+A_2X_2, \tag{1}$$

where, A_{id} is the ideal area per molecule, X_1, X_2 are the mole fraction of the constituent molecules in the mixture, and A_1, A_2 are the values of area per molecule for pure monolayers. One can find the deviation from the ideal behavior by comparing the calculated A_{id} with that obtained experimentally for the mixtures (A_{12}). Figure 12 represents the

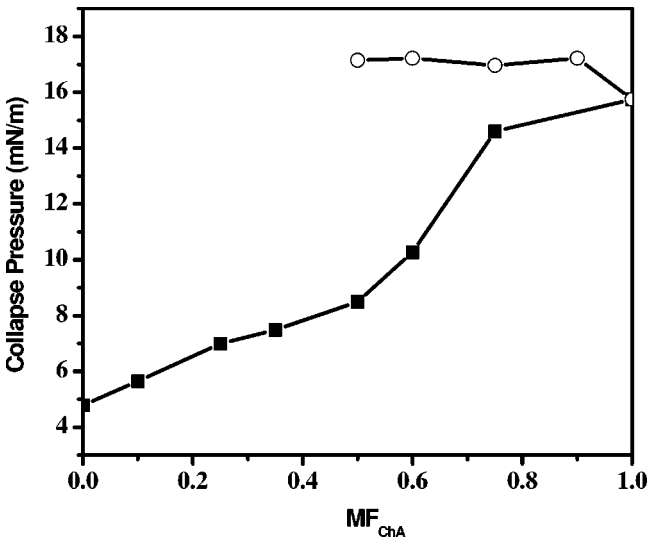

FIG. 11. Variation of collapse pressure as a function of the mole fraction of ChA in ChA-8CB mixed monolayers. The open circles represent the higher collapse pressure $\pi_{c(\mathrm{ChA})}$. The filled squares represent the lower collapse pressure $\pi_{c(8\mathrm{CB})}$.

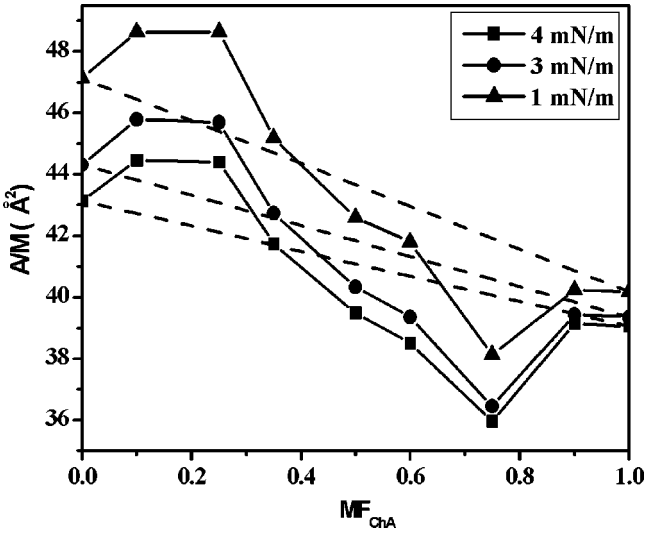

FIG. 12. The variation of the experimentally determined area per molecule A_{12} (continuous lines) and the calculated ideal area per molecule A_{id} (dashed lines) with the mole fraction of ChA in ChA-8CB mixed monolayers at different surface pressures. The difference between A_{12} and A_{id} will give the excess area A_{exc}.

calculated A_{id} and the experimentally determined area per molecule, A_{12} at various surface pressures for the ChA-8CB mixed monolayer. The excess or deficit of area per molecule (A_{exc}) for the mixture from that of the ideal case will indicate the type of interactions. This is given by, $A_{exc}=A_{12}-A_{id}$. The A_{exc} being positive indicates that the interactions are repulsive and the A_{exc} being negative indicates that the interactions are attractive.

The stability of the mixed monolayer was analyzed by calculating the excess Gibbs free energy. The excess Gibbs free energy ΔG_{exc}, for the mixed monolayers at constant surface pressures was obtained by integrating the excess area, A_{exc}, over surface pressure [22]. In its expanded form, ΔG_{exc} is given by

$$\Delta G_{exc}=N_a\int_{\pi^*}^{\pi}(A_{12}-A_1X_1-A_2X_2)d\pi. \tag{2}$$

Here, π^* is the surface pressure at which the two components of the mixed monolayer behave ideally (which is usually taken as zero) and N_a is the Avogadro number. A negative value of the excess Gibbs free energy for the mixed monolayer indicates that the interactions are attractive. On the other hand, if it is positive, then the interactions are of repulsive nature. For the case of the ChA-8CB mixed monolayer, the computed ΔG_{exc} values are depicted in Fig. 13. We can conclude that the interactions are repulsive up to 0.35 MF of ChA and attractive at higher concentrations.

The elastic modulus $|E|$ of the mixed monolayer can be calculated using

$$|E|=(A/M)[d\pi/d(A/M)], \tag{3}$$

where A/M is the area per molecule and π is the surface pressure. For the Ch monolayer, the elastic modulus was found to be 557 mN/m at a surface pressure of 30 mN/m.

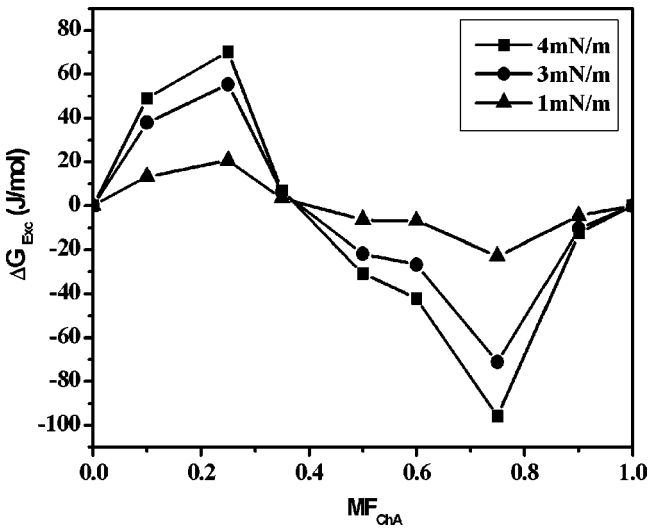

FIG. 13. Variation of excess Gibbs free energy ΔG_{exc} with the mole fraction of ChA in 8CB, computed at different surface pressures.

The elastic modulus for ChA was 460.4 mN/m at a surface pressure of 10 mN/m. The variation of $|E|$ with π in the L_1 phase at different MF of ChA in the ChA-8CB mixed monolayer is shown in Fig. 14. We find an increase in $|E|$ in the mixed monolayer with increasing MF of ChA.

IV. DISCUSSIONS

Our surface manometry experiments showed that the collapse pressures of Ch, ChA, and 8CB were 44.6 mN/m, 15.4 mN/m, and 4.7 mN/m, respectively. The Ch-8CB mixed monolayer exhibited two collapse pressures. The higher collapse pressure $\pi_{c(\mathrm{Ch})}$ was independent of composition. The lower collapse pressure $\pi_{c(8\mathrm{CB})}$ stayed invariant upto 0.6 MF of Ch and then onwards rose steeply. The increase in $\pi_{c(8\mathrm{CB})}$ after 0.6 MF corresponded to the direct transformation of the L_1 phase to the D_2 phase. Based on the surface manometry and epifluorescence microscopic studies on the Ch-8CB mixed monolayer we could characterize the phases. Under the epifluorescence microscope, the L_1 phase exhibits homogeneous intensity and appears very mobile. Thus it is more like a low density liquid phase. The uniformity in the epifluorescence intensity in the L_1 phase is consistent with the Brewster angle microscopy images reported for the 8CB monolayer [19,20,23]. The resulting phase diagram is shown in Fig. 7. In the mixtures, for the composition 0.15 to 0.9 MF of Ch in 8CB, the mixed monolayer exhibited the coexistence of three phases $G+L_1+L_2$. The difference in the dispersion of the dye in the 8CB rich L_1 phase compared to that of the Ch rich L_2 phase might be due to better interaction of the dye with 8CB where it disperses easily into the loosely packed aromatic regions than with the closely packed rigid skeleton of Ch. At lower A/M the monolayer showed that the L_1 and L_2 phases coexist. At still lower A/M, the L_1 phase transformed to the D_1 phase which coexisted with L_2 phase. This trend was seen for the MF in the range 0.15–0.7 of Ch. In the range 0.7–0.9 MF of Ch, the L_1+L_2 coexisting phase transforms into the L_2+D_2 coexisting phase. This direct transformation of L_1 to D_2 corresponds to a kink in the isotherm at about 0.65 MF of Ch. At very low A/M, the L_2 phase collapsed to Ch crystallites. These Ch crystallites coexisted with the D_2 phase. We found that the monolayer exhibited phase separation from 0.15 to 0.9 MF of Ch in 8CB. This indicated that the interaction of Ch and 8CB was weaker. To check the miscibility further, we obtained the π-A/M isotherms for 0.5 MF of Ch in 8CB at 30 °C and 40 °C. Even at these temperatures, there was no appreciable change in the isotherms. Varying the temperature should have affected the interactions like the affinity of the polar head group to the subphase, change in the molecular orientation at the interface, and so on.

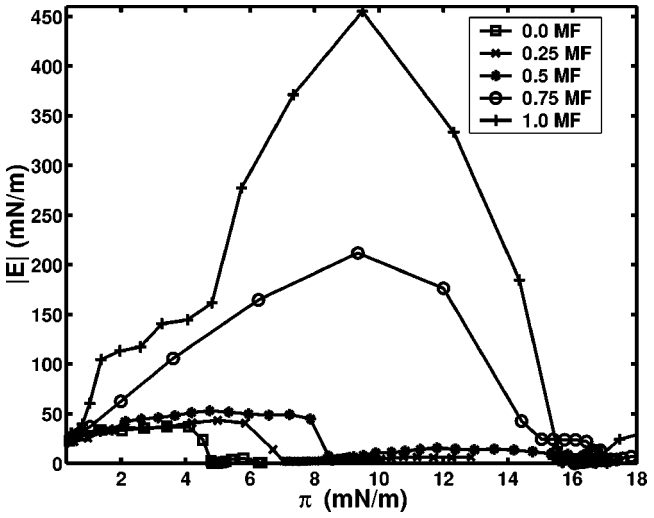

FIG. 14. Variation of the elastic modulus $|E|$ with surface pressure π for systems at different mole fraction of ChA in 8CB.

In Ch monolayer, the rigid skeleton along with OH group is normal to the A-W interface [17]. The OH polar group easily forms hydrogen bonding with water. In the 8CB monolayer, the biphenyl core along with the CN polar group is tilted at the A-W interface [13]. The presence of a strong tilted dipole (CN) alters the local hydrogen bonded network and tends to orient the dipole of water molecules [24]. Such effects have been reported in the case of alkyl cyano biphenyl-water system [25]. This orientational mismatch between OH and CN groups at the A-W interface is the most probable reason for the immiscibility found in our studies in the Ch-8CB mixed monolayer.

A study of mixed monolayers of Ch and stigmastanil phosporylcholine (SPC) in which the rigid skeleton was similar to Ch but with different polar ends has been reported [26]. In the SPC monolayer, the dipole that resides inside the subphase was tilted at an angle of 45° at the interface and the rigid skeleton was oriented normal to the interface. In this Ch-SPC mixed monolayer, the observed miscibility was attributed to the presence of polar OH group of Ch, which decreased the electrostatic repulsion between the SPC dipoles.

In the ChA-8CB mixed monolayer also two collapse pressures were seen. Here the higher collapse pressure $\pi_{c(\mathrm{ChA})}$ was independent of the composition. However, the lower

collapse pressure $\pi_{c(8CB)}$ increased gradually with the concentration of ChA. This behavior was different from that found in the Ch-8CB mixed monolayer. The surface manometry and epifluorescence microscopy studies showed the existence of L_1 phase up to 0.95 MF of ChA. Interestingly, unlike the case of Ch-8CB, there was no phase separation. The phase diagram is shown in Fig. 9. The phases that appeared from 0.1 to 0.25 MF of ChA were $G+L_1$, L_1, L_1+D_1, and L_1+D_2. Here also above $\pi_{c(8CB)}$, the 8CB molecules were squeezed out of the L_1 phase to form multilayers. For a MF of 0.25–0.95 of ChA, the phase sequence was $G+L_1$, L_1, L_1+D_2 and D_2+ChA crystallites.

The ChA molecules are oriented normal at the A-W interface. The presence of OCO group in ChA molecules has the tendency to form weaker hydrogen bonding with water. The degree of hydration or solvation is less for OCO when compared to that of OH. Hence, the OCO group of ChA may laterally interact with the CN group of 8CB and stabilize through dipole-induced dipole interactions. This may favor miscibility in the ChA-8CB mixed monolayer. Surface potential measurements may give more insight into understanding these interactions.

The collapse pressure behavior, similar to that of the ChA-8CB monolayer, has been reported for the case of mixed monolayers of Ch and unsaturated fatty acids [27]. Here also the higher collapse pressure did not vary with the composition and the lower collapse pressure varied with the composition. Further, the degree of unsaturation was varied by choosing molecules with increasing number of double bonds. As the double bonds in the alkyl chain increases, the molecules bend to a greater extent. They had reported that the interactions were stronger for the unsaturated fatty acids, which possessed even numbers of double bonds.

The variation of the elastic modulus $|E|$ with surface pressure for the ChA-8CB monolayer is shown in Fig. 14. The increasing trend in $|E|$ with ChA composition indicated that the mixed monolayer of the ChA-8CB system possesses low in-plane elasticity [28]. Thus the addition of ChA enhances the stability of the 8CB monolayer at the A-W interface. This leads to a comparatively better miscibility for the ChA-8CB mixed monolayer. In the case of the ChA-8CB mixed monolayer, we did not find significant change in the excess area (Fig. 12). The maximum and minimum excess areas were found to be 3 Å^2 and -4 Å^2, respectively. This showed a lower degree of condensation for the mixed monolayer. It also indicated that the presence of either Ch or ChA did not alter the orientation of 8CB molecules drastically.

It may be mentioned that the observations of the phase sequence in the Ch-8CB and ChA-8CB mixed monolayers can be understood in terms of Crisp's phase rule [2,29]. According to this phase rule, the degrees of freedom F for the mixed monolayer at constant temperature and external pressure is

$$F = C_B + C_S - P_B - q + 1, \tag{4}$$

where C_B represents the components in bulk (air and water) and C_S represents the components at the surface (Ch, 8CB or ChA, 8CB). P_B is the number of phases in bulk and q is the number of surface phases. For the Ch-8CB mixed monolayer, $C_B=2$ (air and water), $C_S=2$ (Ch and 8CB), $P_B=3$ (gas, liquid and D_1), and if $q=2$ (L_1 and L_2) then from Eq. (4), $F=0$. This indicates that the collapse pressure is independent of the composition of the mixed monolayer, in agreement with our results up to 0.6 MF of Ch. The change in the collapse pressure after 0.6 MF is due to the transformation of L_1 to D_2 domains. Hence, the Ch-8CB monolayer phase separates in the MF range of 0.15–0.9 of Ch. The component of the monolayer, which had a low value of collapse pressure ($\pi_{c(8CB)}$), gets squeezed out of the mixed monolayer. For the case of the ChA-8CB mixed monolayer, if $C_B=2$ (air and water), $C_S=2$ (ChA and 8CB) and $P_B=3$ (gas, liquid and D_1), then, $F=2-q$. If there is only one monolayer phase ($q=1$) then, $F=1$. This implies that the collapse pressure should vary with the composition of the mixed monolayer in agreement with our results.

V. CONCLUSIONS

Mixed monolayers of Ch and 8CB exhibited the presence of two collapse pressures. The lower collapse pressure varied with composition after 0.6 MF of Ch in 8CB and the higher collapse pressure was independent of the Ch composition. Our epifluorescence studies showed the phase separation of the mixed monolayer into L_1 and L_2 phases in the range 0.15–0.9 MF of Ch in 8CB. In Ch, the OH polar group facilitates hydrogen bonding with water. In 8CB, the strong tilted CN polar group alters the local hydrogen bonded network tending to reorient the dipole of water molecules. This orientational mismatch in hydrogen bonding between the OH and CN groups might have resulted in the observed immiscibility between the Ch and 8CB molecules. The mixed monolayer of ChA-8CB also exhibited two collapse pressures. The lower collapse pressure varied gradually with the concentration of ChA and the higher collapse pressure (as in the previous case) was independent of the composition. From the epifluorescence microscopy, the presence of the L_1 phase was seen up to 0.95 MF of ChA in 8CB and there was no phase separation. Here, the presence of the polar OCO group forms a weaker hydrogen bonding compared to the OH group of Ch. The OCO group may laterally interact with the CN group of 8CB and stabilize the monolayer through dipole-induced dipole interactions. This might have favored better miscibility in the ChA-8CB mixed monolayer when compared to the Ch-8CB system. However, in both these mixed monolayers, above the lower collapse pressure $\pi_{c(8CB)}$, 8CB gets squeezed out, resulting in multilayers.

ACKNOWLEDGMENTS

We are grateful to G. S. Ranganath for helpful discussions.

[1] K.S. Birdi, *Lipid and Biopolymer Monolayers at Liquid Interfaces* (Plenum, New York, 1989).
[2] G.L. Gaines, Jr., *Insoluble Monolayers at Liquid-Gas Interfaces* (Wiley-Interscience, New York, 1966).
[3] K. Simons and E. Ikonen, Science **290**, 1721 (2000).
[4] Y.K. Rao and D.O. Shah, J. Colloid Interface Sci. **137**, 25 (1990).
[5] C.E. McNamee, G.T. Barnes, I.R. Peng, J.H. Steitz, and R. Probert, J. Colloid Interface Sci. **207**, 258 (1998).
[6] R. Seoane, J. Minones, O. Conde, J. Minones, Jr., M. Casas, and E. Iribarnegaray, J. Phys. Chem. B **104**, 7735 (2000).
[7] D. Chapman, N.F. Owens, M.C. Philip, and D.A. Walker, Biochim. Biophys. Acta **183**, 458 (1969).
[8] P. Mattjus, R. Bittman, and J.P. Slotte, Langmuir **12**, 1284 (1996).
[9] L.D. Worthman, K. Nag, P.J. Davis, and K.M.W. Keough, Biophys. J. **72**, 2569 (1997).
[10] M. Sugahara, M. Uragami, X. Yan, and S.L. Regen, J. Am. Chem. Soc. **123**, 7939 (2001).
[11] C. Huang, Nature (London) **259**, 242 (1976).
[12] D.A. Dunmur, M.R. Manterfield, W.H. Miller, and J.K. Dunleavy, Mol. Cryst. Liq. Cryst. **45**, 127 (1978).
[13] J. Xue, C.S. Jung, and M.W. Kim, Phys. Rev. Lett. **69**, 474 (1992).
[14] K.A. Suresh and A. Bhattacharyya, Langmuir **13**, 1377 (1997).
[15] A. Bhattacharyya and K.A. Suresh, Europhys. Lett. **41**, 641 (1998).
[16] I.R. Peterson and R.M. Kenn, Langmuir **10**, 4645 (1994).
[17] H. Rapaport, I. Kuzmenko, H. Berfeld, K. Kjaer, J. Als-Nielsen, R. Popovitz-Biro, I. Weissbuch, M. Lahav, and L. Leiserowitz, J. Phys. Chem. B **104**, 1399 (2000).
[18] C.N. Kwong, R.E. Heikkila, and D.G. Cornwell, J. Lipid Res. **12**, 31 (1971).
[19] M.C. Friedenberg, G.G. Fuller, C.W. Frank, and C.R. Robertson, Langmuir **10**, 1251 (1994).
[20] N.G.M.D. Mul and J.A. Mann, Jr., Langmuir **10**, 2311 (1994).
[21] J.P. Slotte and P. Mattjus, Biochim. Biophys. Acta **1254**, 22 (1995).
[22] F.C. Goodrich, in *Proceedings of the 2nd International Congress on Surface Activity*, edited by J.H. Schulman (Butterworths, London, 1957), Vol. 1, p. 85.
[23] J. Lauger, C.R. Robertson, C.W. Frank, and G.G. Fuller, Langmuir **12**, 5630 (1996).
[24] D. Chandler, Nature (London) **417**, 491 (2002).
[25] X. Zhuang, D. Wilk, L. Marrucci, and Y.R. Shen, Phys. Rev. Lett. **75**, 2144 (1995).
[26] R. Seoane, J. Minones, O. Conde, and J. Minones, Jr., Colloids Surf., A **174**, 329 (2000).
[27] R. Seoane, J. Minones, Jr., P. Dynarowicz-tstka, and I. Rey-Gomez-Serranillos, Colloid Polym. Sci. **279**, 562 (2001).
[28] X. Li, M.M. Momsen, J.M. Smaby, H.L. Brockman, and R.E. Brown, Biochemistry **40**, 5954 (2001).
[29] D.J. Crisp, *Surface Chemistry*, Suppl. to Research (Butterworths, London, 1949), p. 17.